

Physics-Based Optimal Controls

7.1: Degradation as basis for power limits

- We now approach the frontier of knowledge in battery management:
 - The electronics aspects are important, but routine;
 - State-of-charge is well defined, and established methods can be used to get good SOC estimates;
 - Similarly, we have seen good methods to estimate resistance and total capacity of cells, yielding state-of-health estimates;
 - Cell energy calculation is straightforward; and
 - Several types of cell balancing—with varying complexities and speed—can be implemented.
- Improvements can yet be made to all of the above, but the present state of the art provides adequate BMS for many applications.
 - Some questions regarding long-term efficacy of present BMS on aged battery packs;
 - Other issues regarding power calculation, as described in this chapter.
- “Using current electronics and knowledge it takes about two years and \$250K to build a custom BMS” [Davide Andrea].
 - Not trivial, but very doable.

More power!

- The big pink elephant in the room that few people talk about is the way that power estimates are presently calculated.
- The premise behind these methods is that voltage limits must never be violated.
- But why? The real issue is cell degradation. The assumption is that:
 - If voltage limits are violated, then the cell will degrade quickly;
 - If limits are properly maintained, the cell will have a long and productive and happy life.
- But, in fact, voltage limits **may** be violated for a short time in some situations without causing any faster aging.
- And, “normal” voltages may also cause fast degradation in some situations—particularly for an aged cell.
- So, real issue is not cell voltage but rather rate of aging/degradation.
- Cell power limits **should** really be calculated to more directly optimize a tradeoff between performance delivered by the cell and the rate of incremental degradation experienced by the cell.
- To be able to do this, we must be able to:
 1. Model degradation mathematically, and
 2. Devise model-based optimized controls to calculate best tradeoff.
- Some have suggested that if this is done perfectly, battery-pack sizes may be reduced by up to 50 %, yet still deliver required performance.
 - This is ample incentive to make a strong attempt.

Modeling cell degradation

- We have seen that much is known about cell degradation qualitatively.
- But, how about quantitatively? That is, can we make accurate mathematical models of all the degradation mechanisms?
- We have seen that interactions between mechanisms are complex. Further, they are not presently well understood.
 - Philosophy = “a blind man searching in a dark room for a black cat that isn’t there.” Are we on the same kind of futile search?
- At this point, we don’t know. (That’s the nature of research!)
- But, working in our favor is that we don’t need to model **all** mechanisms **perfectly** to have a useful result.
 - For purposes of control, we don’t need to model any mechanism that is not influenced by a variable that we have control over;
 - If we model the most severe mechanisms reasonably well, then we have a chance at designing controls that make a difference.

Literature that proposes models of degradation

- The literature on degradation mechanism modeling is quite sparse.
- Here, we look at two models: SEI formation/growth; lithium plating.

7.2: Full-order model of SEI formation and growth

- Ramadass and colleagues have proposed a model that describes the formation and growth of an SEI layer on negative-electrode solid particles during charging, that uses solvent reduction as the main side reaction mechanism for degradation (Ramadass 2004).
- Here, we build on that work to develop a simple incremental model of SEI growth and associated capacity loss and resistance rise.¹
- The order-reduction method uses volume averaging to create an algebraic “0-D” model of the infinite-order PDE model.
- This reduced-order model (ROM) of the SEI growth mechanism is a first step toward creating a complete coupled reduced-order model of all dominant cell degradation mechanisms, which then could be used in an optimal control scheme.

Original model

- Changes at the electrode/electrolyte interface due to side reactions at the negative electrode are considered to be one of the primary causes of cell aging.
- There are a large number of reduction reactions that can lead to the deposition of solid SEI products on the electrode surface, and these are less well understood, being very dependent upon the composition of the electrolyte solution.

¹ Adapted from, Randall, A.V., Perkins, R.D., Zhou, X., Plett, G.L., “Controls Oriented Reduced Order Modeling of SEI Layer Growth,” *Journal of Power Sources*, Vol. 209, July 2012, pp. 282–288.

- Ramadass makes general assumptions that the side reaction is considered to be a consumption of the solvent species and lithium ions, which will form compounds such as Li_2CO_3 , LiF , Li_2O , and so forth, depending on the nature of the solvent.
- There is significant porosity in the film, and this makes it reasonable to assume that the SEI layer continues to grow as the solvent diffuses through the layer during charge.
- The assumption of the ongoing formation of the SEI layer is also supported by the research of Aurbach and colleagues (1999), who propose that the intercalation of lithium into the graphite negative electrode leads to increase in the lattice volume, which in turn stretches the SEI layer, causing it to fracture and to expose more of the active material to the electrolyte, fueling the side reaction, and contributing to SEI formation.
- Ramadass' model assumes:
 1. The main side reaction is due to the reduction of an organic solvent, expressed as $\text{S} + 2\text{Li}^+ + 2e^- \rightarrow \text{P}$, where "S" refers to the solvent and "P" to the product formed in the side reaction.
 2. The reaction occurs only during charging of the cell.
 3. The products formed are a mixture of different species, resulting in averaged mass and density constants used in the later equation describing the formation and growth of the SEI film.
 4. The side reaction is assumed to be irreversible and U_s^{ref} is chosen to be 0.4 V versus Li/Li^+ .
 5. The initial resistance of the SEI layer developed during cell formation is $0.01 \Omega\text{m}^2$.

6. There is no overcharge reaction considered (*i.e.*, lithium plating is not modeled).
- We have somewhat relaxed assumption 2, allowing side reactions to occur during rest intervals also (and even during discharge).
 - The SEI growth model is tightly coupled with a Newman-style physics-based model of ideal-cell dynamics.
 - For the negative electrode, the local molar flux j_{total} is given by a sum of the intercalation flux j and the side reaction flux j_s ,

$$j_{\text{total}} = j + j_s,$$

where j is computed via the Butler–Volmer electrochemical kinetic expression

$$j = \frac{i_0}{F} \left[\exp\left(\frac{\alpha_a F}{RT} \eta\right) - \exp\left(-\frac{\alpha_c F}{RT} \eta\right) \right],$$

which is driven by the overpotential

$$\eta = \phi_s - \phi_e - U_n^{\text{ref}} - FR_{\text{film}} j_{\text{total}},$$

where i_0 [A m^{-2}] is the exchange current density and U_n^{ref} is the equilibrium potential in the negative electrode, evaluated as a function of the solid-phase concentration at the surface of the particle.

- The kinetics of the side reaction are described using a Tafel equation, which assume that the side reaction is considered irreversible,

$$j_s = -\frac{i_{0,s}}{F} \exp\left(-\frac{\alpha_s F}{RT} \eta_s\right),$$

and the side reaction overpotential is described as

$$\eta_s = \phi_s - \phi_e - U_s^{\text{ref}} - FR_{\text{film}} j_{\text{total}}.$$

- Once the side reaction flux, j_s , has been calculated, the change in the film thickness δ_{film} during charging can be calculated by

$$\frac{\partial \delta_{\text{film}}}{\partial t} = -\frac{M_P}{\rho_P} j_s,$$

where M_P [kg mol⁻¹] is the average molecular weight of the constituent compounds of the SEI layer and ρ_P [kg m⁻³] is the average density of the constituent compounds.

- This allows the overall film resistance to be calculated as

$$R_{\text{film}} = R_{\text{SEI}} + \delta_{\text{film}}/\kappa_P,$$

where R_{SEI} is the initial film resistance that is produced during the formation period of the cell, and κ_P [S m⁻¹] is the conductivity of the film.

- In addition to the resistance change, there is a capacity loss caused by the side reaction current during charge, leading to capacity changing via the relationship

$$\frac{\partial Q}{\partial t} = \int_0^{L_n} a_n A F j_s dx.$$

7.3: Simplifying the model

- To effect an optimal control strategy, the battery management system must be able to calculate the side reaction flux j_s very quickly and accurately.
- Solving the coupled PDE equations described above (plus the physics-based ideal-cell model) is too complicated for such a process.
- The j_s model needs to be much faster and simpler. In this section, we present a simpler incremental model for calculating j_s , R_{film} , and Q .
- To create a volume-averaged 0-D reduced-order model, three additional assumptions are made:
 1. The cell is always in a quasi-equilibrium state, allowing the exchange current density i_0 to be calculated from the cell SOC alone, neglecting local variations in electrolyte and solid surface concentration. The estimated value of j_s then corresponds to a suddenly applied current pulse $i_{\text{app}}(t)$, which is constant over some time interval Δt .
 2. The intercalation and the side-reaction fluxes are uniform over the negative electrode. This allows us to state that the total reaction flux j_{total} is related to the applied cell current i_{app} by the following relationship:

$$j_{\text{total}} = \frac{i_{\text{app}}}{a_n F \text{Vol}_n},$$
 where the volume of the active material is described by $\text{Vol}_n = L_n A$.
 3. The anodic and cathodic charge-transfer coefficients are equal ($\alpha_a = \alpha_c = 0.5$).

- From the above assumptions, an incremental degradation model can be formulated as follows. First, at any point in time, the lithiation state of the negative electrode is calculated as

$$\theta_n = \theta_{n,\min} + \text{SOC}_{\text{cell}} (\theta_{n,\max} - \theta_{n,\min}),$$

where:

- $\theta_{n,\max}$ and $\theta_{n,\min}$ are the stoichiometric limits of negative-electrode lithiation (*i.e.*, the value of θ in $\text{Li}_\theta\text{C}_6$ when the cell is fully charged and discharged, respectively).
- SOC_{cell} is a value between zero and one, which indicates the cell state-of-charge.
- Then U_n^{ref} is calculated from θ_n for the electrode materials being used.
- We will ultimately iterate to find j_s . We can initialize its value to zero and calculate the intercalation flux:

$$\begin{aligned} j &= j_{\text{total}} - j_s \\ &= \frac{i_{\text{app}}}{a_n F \text{Vol}_n} - j_s. \end{aligned}$$

- From j and assumption 3,

$$\begin{aligned} j &= \frac{i_0}{F} \left[\exp\left(\frac{F}{2RT}\eta\right) - \exp\left(-\frac{F}{2RT}\eta\right) \right] \\ &= \frac{2i_0}{F} \sinh\left(\frac{F}{2RT}\eta\right) \\ \eta &= \frac{2RT}{F} \text{asinh}\left(\frac{Fj}{2i_0}\right). \end{aligned}$$

- Then, we note the similarity between the expressions for η and η_s to find:

$$\begin{aligned}\eta &= \phi_s - \phi_e - U_n^{\text{ref}} - FR_{\text{film}}j_{\text{total}} \\ \eta_s &= \phi_s - \phi_e - U_s^{\text{ref}} - FR_{\text{film}}j_{\text{total}} \\ &= \eta + U_n^{\text{ref}} - U_s^{\text{ref}} \\ &= \frac{2RT}{F} \operatorname{asinh} \left(\frac{Fj}{2i_0} \right) + U_n^{\text{ref}} - U_s^{\text{ref}}.\end{aligned}$$

- The film resistance cancels from the calculation. We can now calculate an updated estimate of the side-reaction flux as

$$j_s = -\frac{i_{0,s}}{F} \exp \left(\frac{-F}{2RT} \eta_s \right).$$

- In total, we have the reduced-order model

$$\begin{aligned}j_s &= -\frac{i_{0,s}}{F} \exp \left(\frac{-F}{2RT} \left(\frac{2RT}{F} \operatorname{asinh} \left(\frac{Fj}{2i_0} \right) + U_n^{\text{ref}} - U_s^{\text{ref}} \right) \right) \\ &= -\frac{i_{0,s}}{F} \exp \left(\frac{-F}{2RT} \left(\frac{2RT}{F} \operatorname{asinh} \left(\frac{F \left(\frac{i_{\text{app}}}{a_n F \text{Vol}_n} - j_s \right)}{2i_0} \right) + U_n^{\text{ref}} - U_s^{\text{ref}} \right) \right) \\ &= -\frac{i_{0,s}}{F} \exp \left(\frac{F (U_s^{\text{ref}} - U_n^{\text{ref}})}{2RT} \right) \exp \left(\operatorname{asinh} \left(\frac{\frac{-i_{\text{app}}}{a_n \text{Vol}_n} + Fj_s}{2i_0} \right) \right).\end{aligned}$$

- We'll see how to solve this equation for j_s shortly.
- Once we have solved for j_s it can then be incorporated into incremental equations for film resistance and capacity loss.
- It is assumed that j_s is constant over some small time interval Δt , and is denoted as $j_{s,k}$ for the k th interval.
- We can convert the continuous-time film thickness relationship to discrete time as:

$$\frac{\partial \delta_{\text{film}}}{\partial t} = -\frac{M_P}{\rho_P} j_s$$

$$\delta_{\text{film},k} = \delta_{\text{film},k-1} - \frac{M_P \Delta t}{\rho_P} j_{s,k-1},$$

noting that the sign of j_s is negative.

- This result can be used to calculate the film resistance as

$$R_{\text{film}} = R_{\text{SEI}} + \delta_{\text{film}}/\kappa_P$$

$$R_{\text{film},k} = R_{\text{film},k-1} - \frac{M_P \Delta t}{\rho_P \kappa_P} j_{s,k-1}.$$

- Similarly, we can discretize the capacity equation

$$\frac{\partial Q}{\partial t} = \int_0^{L_n} a_n A F j_s dx$$

$$Q_k = Q_{k-1} + (a_n A F L_n \Delta t) j_{s,k-1}.$$

- In summary, the proposed reduced-order model (ROM) equations are:

$$\theta_n = \theta_{n,\min} + \text{SOC}_{\text{cell}} (\theta_{n,\max} - \theta_{n,\min})$$

$$j_{s,k} = -\frac{i_{0,s}}{F} \exp\left(\frac{F (U_s^{\text{ref}} - U_n^{\text{ref}})}{2RT}\right) \exp\left(\text{asinh}\left(\frac{\frac{-i_{\text{app}}}{a_n \text{Vol}_n} + F j_{s,k}}{2i_0}\right)\right),$$

$$R_{\text{film},k} = R_{\text{film},k-1} - \frac{M_P \Delta t}{\rho_P \kappa_P} j_{s,k-1}$$

$$Q_k = Q_{k-1} + (a_n A F L_n \Delta t) j_{s,k-1}.$$

7.4: Simplifying the calculation

- As it is written now, $j_{s,k}$ is an implicit calculation

$$j_{s,k} = -\frac{i_{0,s}}{F} \exp\left(\frac{F(U_s^{\text{ref}} - U_n^{\text{ref}})}{2RT}\right) \exp\left(\text{asinh}\left(\frac{\frac{-i_{\text{app}}}{a_n \text{Vol}_n} + F j_{s,k}}{2i_0}\right)\right).$$

- One solution methodology would be to use iteration:
 1. Guess a value for $j_{s,k}$ (e.g., zero),
 2. Plug in to RHS of relationship; calculate LHS as new value for $j_{s,k}$,
 3. Repeat step 2 until no significant change in $j_{s,k}$.
- This method actually works pretty well, and we can arrive at a solution in fewer than 10 iterations.
- However, there is also a closed-form solution for $j_{s,k}$ (not obvious).
- First, let's simplify notation:

$$j_{s,k} = \underbrace{-\frac{i_{0,s}}{F} \exp\left(\frac{F(U_s^{\text{ref}} - U_n^{\text{ref}})}{2RT}\right)}_A \exp\left(\text{asinh}\left(\underbrace{\frac{-i_{\text{app}}}{2a_n i_0 \text{Vol}_n}}_B + \underbrace{\frac{F}{2i_0} j_{s,k}}_C\right)\right)$$

$$= A \exp(\text{asinh}(B + C j_{s,k})).$$

- Note that $A < 0$ and $C > 0$ always.
- Also note that the value of A can be stored in a lookup table versus θ_n , so is not difficult to calculate in real time.
- A useful identity for simplifying this further is:

$$\exp(\text{asinh}(x)) = x + \sqrt{x^2 + 1}.$$

- So, we can write

$$j_{s,k} = A \left[(B + Cj_{s,k}) + \sqrt{(B + Cj_{s,k})^2 + 1} \right]$$

$$\frac{j_{s,k}}{A} - B - Cj_{s,k} = \sqrt{(B + Cj_{s,k})^2 + 1}$$

$$j_{s,k}(1 - CA) - AB = A\sqrt{(B + Cj_{s,k})^2 + 1}$$

$$(j_{s,k}(1 - CA) - AB)^2 = A^2(B + Cj_{s,k})^2 + A^2$$

$$0 = A^2(B + Cj_{s,k})^2 + A^2 - (j_{s,k}(1 - CA) - AB)^2$$

$$= A^2(B^2 + 2BCj_{s,k} + C^2j_{s,k}^2) + A^2$$

$$- (j_{s,k}^2(1 - CA)^2 - 2AB(1 - CA)j_{s,k} + A^2B^2).$$

- Collecting like terms

$$0 = (A^2C^2 - (1 - CA)^2)j_{s,k}^2 + (2A^2BC + 2AB(1 - CA))j_{s,k} + (A^2B^2 + A^2 - A^2B^2).$$

- Note that $(1 - CA)^2 = 1 - 2CA + A^2C^2$, so this simplifies,

$$0 = (2CA - 1)j_{s,k}^2 + (2AB)j_{s,k} + (A^2).$$

- Key point: This is a quadratic, so we can easily solve for the root(s) using the quadratic formula:

$$\begin{aligned} j_{s,k} &= \frac{-2AB \pm \sqrt{4A^2B^2 - 4A^2(2CA - 1)}}{2(2CA - 1)} \\ &= \frac{AB \pm A\sqrt{B^2 + (1 - 2CA)}}{(1 - 2CA)}. \end{aligned}$$

- But, which root to use? The Routh test gives us some guidance:

$$\begin{array}{l|l} j_{s,k}^2 & 2CA - 1, \quad A^2 \\ j_{s,k} & 2AB \\ 1 & A^2 \end{array}$$

- Since $2CA - 1 < 0$ and $A^2 > 0$, we are guaranteed two sign changes, which means that this equation always has exactly one positive real root and one negative real root.
- Physically, we know that $j_{s,k} < 0$ (because $A < 0$), so we want to take the smaller root of the quadratic solution.
- So, because $A < 0$,

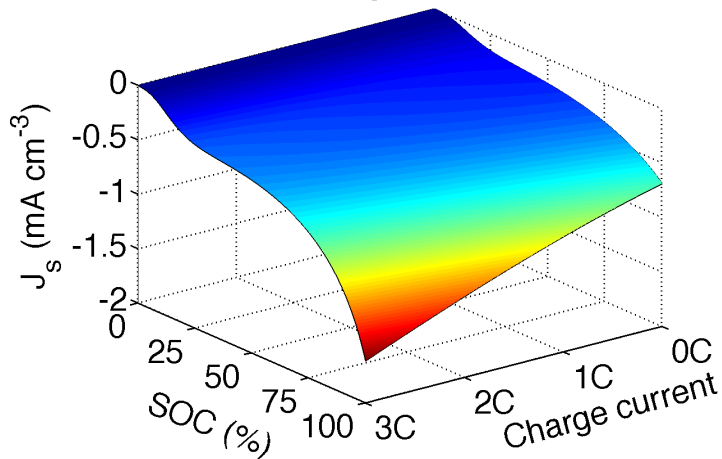
$$j_{s,k} = \frac{AB + A\sqrt{B^2 + (1 - 2CA)}}{(1 - 2CA)}.$$

7.5: Comparing the models

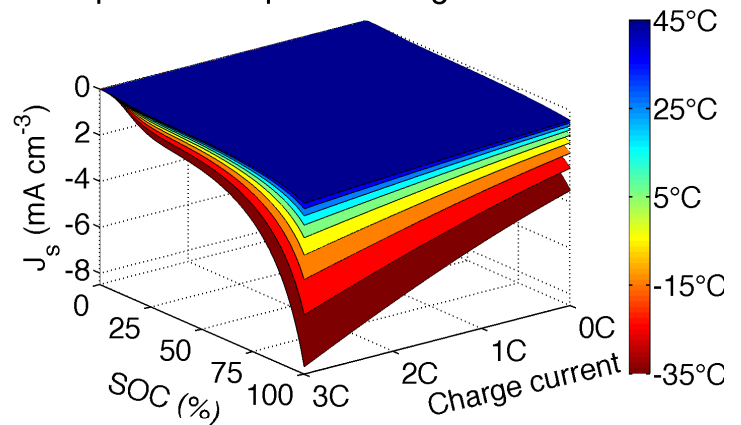
- The validity of this reduced-order model depends first on the accuracy of the underlying partial differential equation model, which we assume here to be exact.
- It then depends on how closely the reduced-order approximation of j_s matches the exact calculation of j_s .
- To compare the PDE and reduced-order models, we conducted a series of simulations.
 - In each simulation, the cell was initially at rest.
 - A sudden pulse of current was then applied, and the instantaneous resulting j_s from the PDE model was compared to the computed j_s from the ROM.
- To simulate the PDE model, we used COMSOL Multiphysics 3.5a coupled with a MATLAB script to cycle through the series of simulations and analyze results.
 - Specifically, each simulation comprised a 1 s time interval, where the cell current i_{app} was modeled as a Heaviside step function, which was applied half-way through the interval.
 - We found that the initial rest interval facilitated convergence of the solution by allowing the PDE solver to adjust its initial conditions before applying the step current.
- The simulation cell parameters that we used are listed in the appendix. In particular, the cell had a 1.8 Ah capacity.
- For the full-order PDE simulations:

- Applied current was varied from 0 A to 5.4 A in steps of 0.1 A;
 - Initial cell SOC was varied from 0 % to 100 % in steps of 2 %; and
 - Temperature was varied from -35°C to 45°C in steps of 20°C .
- For the reduced-order simulations, which run much more quickly:
 - Applied current was varied from 0 A to 5.4 A in steps of 0.05 A;
 - Initial cell SOC was varied from 0 % to 100 % in steps of 1 %; and
 - Temperature was varied from -35°C to 45°C in steps of 10°C .
 - As one point of comparison, the set of 14 025 full-order PDE simulations took more than eight days to complete on an Intel i7 processor, while the set of 112 200 ROM simulations took a total of about 2.6 seconds to complete on the same machine.
 - The speedup, on a per-simulation basis, is more than 2 000 000 : 1. This is the primary advantage of the ROM over the PDE model.
 - The figure below-left shows room-temperature side-reaction flux j_s as computed by the reduced-order model (which we now denote as $j_{s,\text{ROM}}$).
 - The figure below-right shows a compilation of $j_{s,\text{ROM}}$ over a range of temperatures. We see two trends that match experience: degradation is worst at high SOC and high charge rates.

Instantaneous degradation rate, 25°C

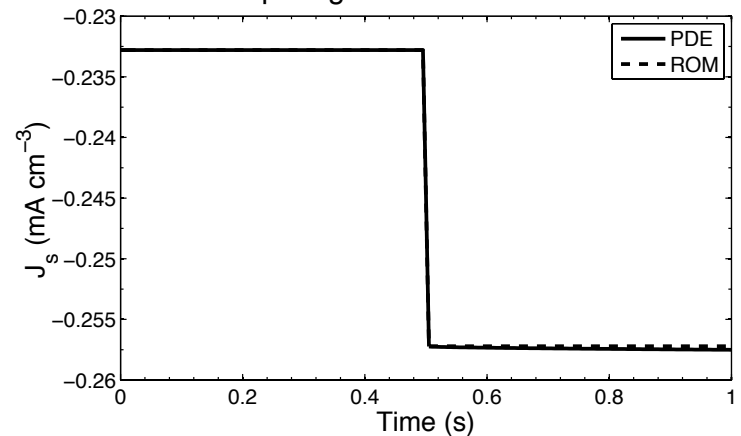


Temperature dependent degradation rate



- The figure to the right shows results of one PDE simulation.
- This example was conducted at 25 °C, 50 % SOC, and by applying a 1C charge pulse at $t = 0.5$ s.
- The figure shows the raw output of the simulation, as compared to the ROM.
- Both the PDE and ROM solutions have a non-zero negative side reaction flux j_s even when the cell is at rest.
- This is due to the fact that we have relaxed assumption 2 of the SEI growth model to also allow for the side reaction when current in the external circuit is zero.
- The figure shows that the ROM matches both the rest SEI side-reaction rate and the charge-pulse SEI side-reaction rate.
- Plotted on the same scale, the full PDE solution results are indistinguishable from the ROM results. So, for comparison purposes,

Comparing ROM to PDE solutions

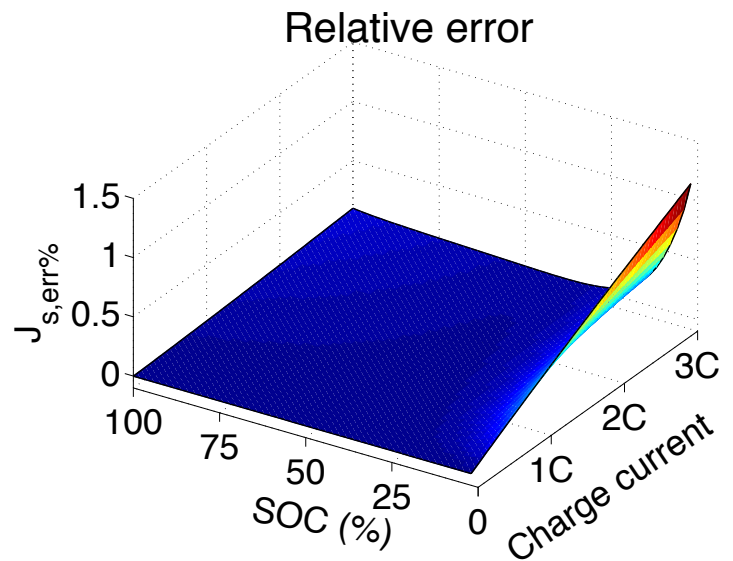


we define a relative error between the results as

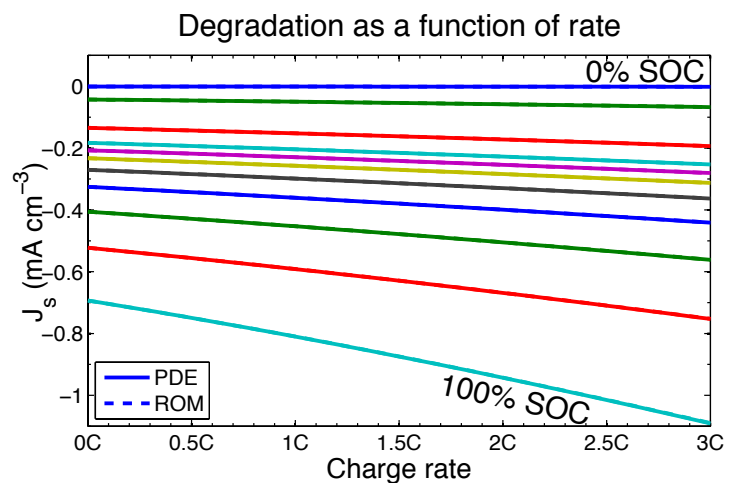
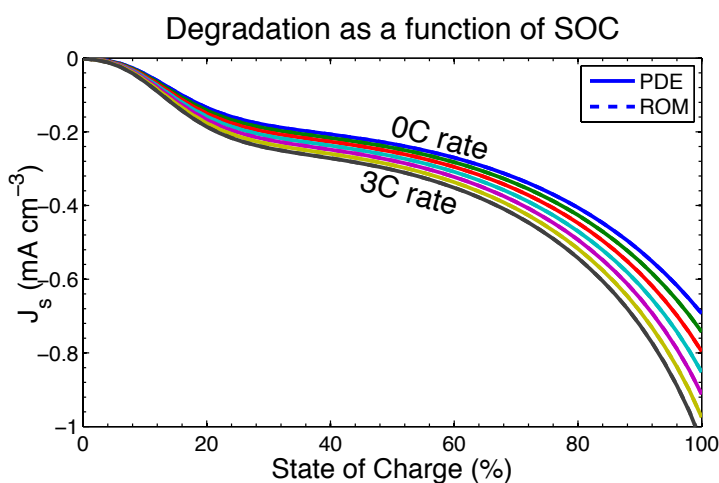
$$j_{s, \text{err}\%} = \frac{j_{s, \text{PDE}} - j_{s, \text{ROM}}}{j_{s, \text{PDE}}} \times 100,$$

where $j_{s, \text{PDE}}$ is chosen to be the value of j_s from the PDE solution immediately after the application of the current pulse.

- The figure plots the relative error between the PDE and ROM solutions for all 25 °C simulations.
- Between 10 % and 90 % SOC (e.g., typical extremum operating conditions for EV cells), the maximum relative error was 0.44 %.



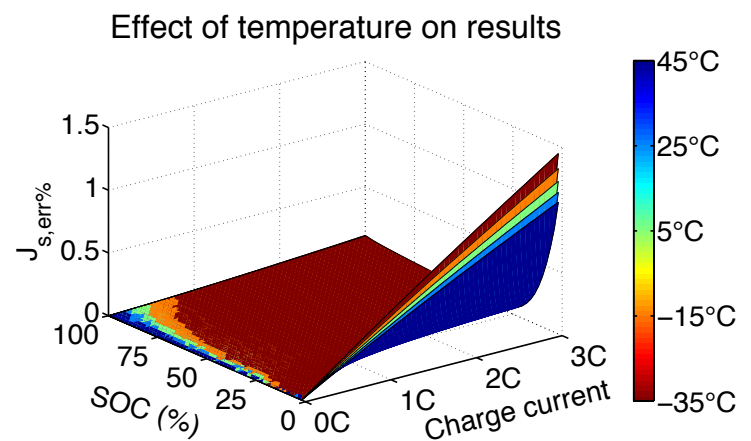
- To further illustrate the performance of the ROM and to see the dependence of SEI layer growth rate on SOC and charge rate, the figures below plot these results in a different format (25 °C).



- The left frame shows j_s as a function of SOC at different charge rates (lines plotted from 0C to 3C in steps of 0.5C).

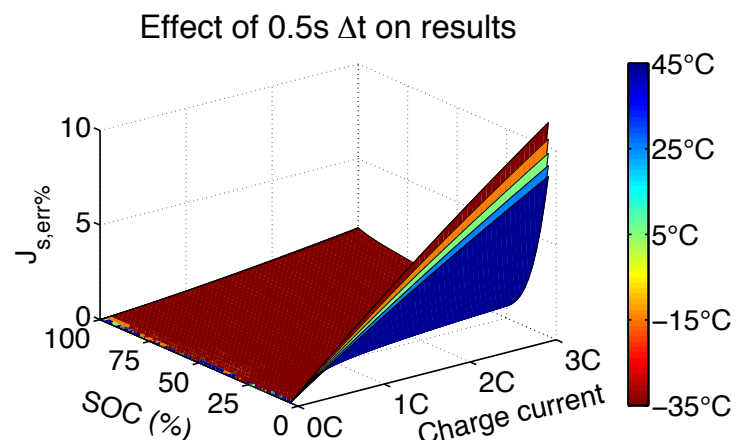
- The right frame shows j_s as a function of charge rate at different SOC's (plotted from 0 % SOC to 100 % SOC in steps of 10 % SOC).
- In all plots, the corrected PDE result is drawn as a solid line, and the ROM result is drawn as a dashed line. In most cases, it is impossible to visually distinguish between the PDE and ROM results.
- The figures below show additional effects on relative error. First, we see how error varies with temperature.
- The ROM predictions are best at high temperatures, and less good at low temperatures.

- Worst-case $j_{s,err\%}$ in the 10 % to 90 % SOC range varies from 0.41 % at 45 °C to 0.55 % at -35 °C.



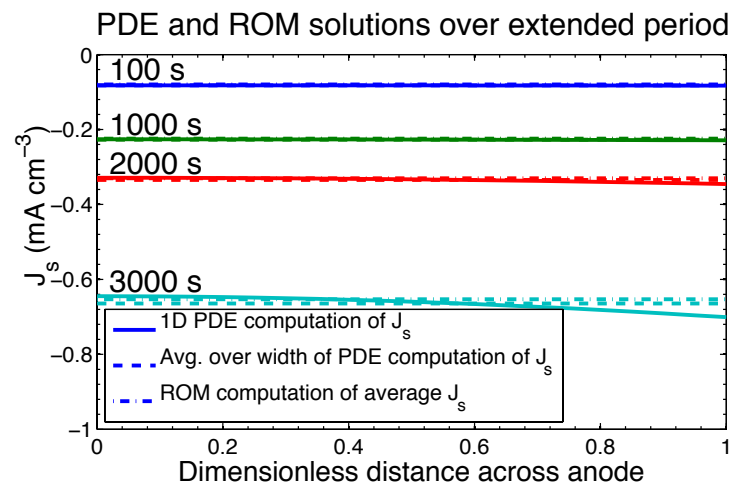
- Next, we investigate the effect of Δt on the results. Instead of selecting the value for $j_{s,PDE}$ immediately after the application of the current pulse, $j_{s,PDE}$ is now selected to be the PDE solution 0.5 s seconds after the application of the current pulse, at the $t = 1$ s point.

- The relative error is once again worst at low temperatures and low values of SOC (where the absolute amount of degradation is small).



- Relative errors over 10 % are observed in some cases, but in the ranges of SOC most important for control, where SOC is greater than 25 %, the worst-case $j_{s, \text{err}\%}$ is far less, varying from 0.85 % at 45 °C to 1.04 % at –35 °C.

- The figure to the right investigates the effect of a prolonged constant-current charge at a 1C rate, as might be experienced when a cell is being charged.



- The PDE is simulated for 3 000 s, starting with the cell at rest at 10 % SOC, and 1D profiles of $j_s(x)$ across the negative electrode are plotted at time steps 100 s, 1 000 s, 2 000 s, and 3 000 s.
- Overlaid on the plot are the average j_s values predicted by the ROM at that SOC level, and the actual averaged j_s values (averaged over the 1D electrode) from the PDE solution.
- In the ROM simulation, the SOC is updated on a second-by-second basis to achieve the present SOC at every point, which is used to compute the value of j_s using the method explained herein.
- We see that even over prolonged constant-current charge profiles, the ROM is accurate, indicating that assumption 1 of ROM is a reasonable assumption to make.

7.6: Lithium deposition on overcharge

- The success of the preceding ROM to predict the performance of a Tafel equation leads us to expect it will work well for other similar aging mechanisms (*e.g.*, Darling and Newman, 1998).
- The PDE model of lithium deposition on overcharge by Arora *et al.*, however, does not use a Tafel equation.
 - Instead, it uses a modified Butler–Volmer equation.
- Here, we address creation of a ROM of lithium deposition on overcharge.²
 - It does not work as well as the SEI ROM, especially for prolonged charging events.
 - It is probably better suited for predicting degradation in an HEV scenario, with random charges.
 - We’re working on another method right now, that we think will work better, but it isn’t ready for public consumption as yet.
- Lithium deposition/plating is not usually considered a dominant degradation mechanism, because the cell terminal voltage limits are designed to avoid conditions that would be conducive to plating.
 - However (especially at cold temperatures), the terminal voltages are poor indicators of internal cell potentials,
 - Plating can still happen, and when it does, there is immediate severe capacity loss.

² Adapted from, Perkins, R.D., Randall, A.V., Zhou, X., Plett, G.L., “Controls Oriented Reduced Order Modeling of Lithium Deposition on Overcharge,” *Journal of Power Sources*, Vol. 209, July 2012, pp. 318–325.

- So, modeling lithium deposition is very important to be able to devise optimized controls to minimize aging.
- Overcharge manifests first as a metallic lithium deposit on the surface of the negative electrode solid particles during charge, predominantly near the separator.
- Subsequently, the lithium can and does further combine with electrolyte material to form other compounds such as Li_2O , LiF , Li_2CO_3 , and polyolefins.
- The nature of the final product is not our major concern; rather, the issue is that lithium is irreversibly lost.
- This phenomenon is an unintended side reaction that can lead to severe capacity fade, electrolyte degradation, possible safety hazard.

Physics-based model of overcharge

- This work is based on a physics-based model proposed by Arora *et al.* (1999).
- Our goal is to create a high-fidelity reduced-order model of this PDE degradation model; therefore, we adopt the same assumptions as they, which were:
 1. The main side reaction is expressed as $\text{Li}^+ + \text{e}^- \rightarrow \text{Li}(\text{s})$, which occurs at $U_s^{\text{ref}} = 0 \text{ V}$ versus Li/Li^+ during an overcharge event. This lithium metal is expected to form first near the electrode-separator boundary where the surface overpotential is greatest.
 2. Lithium metal deposited on the negative electrode reacts quickly with solvent or salt molecules in the vicinity, yielding Li_2CO_3 , LiF , or

other insoluble products. A thin film of these products protects the solid lithium from reacting with the electrolyte. Solid lithium can still dissolve during discharge, but once lithium is consumed in a insoluble product, it is permanently lost.

3. The insoluble products formed are a mixture of different species, resulting in averaged mass and density constants used in a later equation describing the formation and growth of a resistive film.
 4. Only the overcharge reaction is considered (*e.g.*, SEI film growth and other degradation mechanisms are not modeled).
- The overcharge model of Arora is tightly coupled with a “pseudo two-dimensional” Newman-style porous-electrode style model of ideal-cell dynamics.
 - In the ideal cell, intercalation flux $j(x, t)$ is expressed as the Butler–Volmer equation,

$$j(x, t) = \frac{i_0}{F} \left[\exp \left(\frac{\alpha_{a,n} F}{RT} \eta(x, t) \right) - \exp \left(-\frac{\alpha_{c,n} F}{RT} \eta(x, t) \right) \right]$$

which is driven by the overpotential

$$\eta(x, t) = \phi_s(x, t) - \phi_e(x, t) - U_n^{\text{ref}} - FR_{\text{film}} j(x, t),$$

where i_0 is the exchange current density,

$$i_0 = k_n (c_{s,n}^{\text{max}} - c_{s,n})^{\alpha_{a,n}} (c_{s,n})^{\alpha_{c,n}} (c_e)^{\alpha_{a,n}},$$

and U_n^{ref} is the equilibrium potential which is evaluated as a function of the solid phase concentration at the surface of the particle.

- Arora expresses the side-reaction flux j_s (*i.e.*, the rate of irreversible lithium loss due to lithium plating) as

$$j_s(x, t) = \min \left(0, \frac{i_{0,s}}{F} \left[\exp \left(\frac{\alpha_{a,s} F}{RT} \eta_s(x, t) \right) - \exp \left(- \frac{\alpha_{c,s} F}{RT} \eta_s(x, t) \right) \right] \right),$$

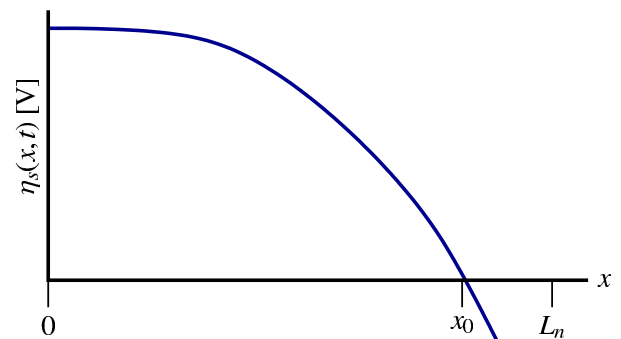
where $\alpha_{a,s} \neq \alpha_{c,s}$ in general,

$$\eta_s(x, t) = \phi_s(x, t) - \phi_e(x, t) - U_s^{\text{ref}} - FR_{\text{film}} j_s(x, t),$$

and where the side-reaction exchange current density

$$i_{0,s} = k_{n,s} (c_e)^{\alpha_{a,s}}.$$

- Side reaction is semi-irreversible in the sense that it includes an anodic rate term, but doesn't allow overall positive side-reaction flux.
- The side reaction occurs only at spatial locations in the negative electrode where $\eta_s(x, t) < 0$.
- This is enforced in the j_s equation by the “min” function, which sets $j_s(x, t) = 0$ for values of x where $\eta_s(x, t) \geq 0$, but to the value computed by the Butler–Volmer equation when $\eta_s(x, t) < 0$.
- A typical scenario is plotted in the figure, where $\eta_s(x, t)$ is sketched across the electrode width.
- In this example, plating will occur in the interval from $x = x_0$ to $x = L_n$.
- Note that this illustration shows that the cell can be quite far away from 100 % state-of-charge and still have plating occur near the separator if a large enough charge-current pulse is applied to the cell's terminals.
 - The state-of-charge is only one variable of importance—ultimately, the local overpotential determines whether plating occurs.



- So, our first goal will be to solve for j_s . Then, once we have solved for j_s , it can then be incorporated into incremental equations for film resistance and capacity loss.
- We assume that j_s is constant over some small time interval Δt , and denote it as $j_{s,k}$ for the k th interval.
- We can convert the continuous-time film thickness relationship to discrete time as:

$$\frac{\partial \delta_{\text{film}}}{\partial t} = -\frac{M_P}{\rho_P} j_s$$

$$\delta_{\text{film},k} = \delta_{\text{film},k-1} - \frac{M_P \Delta t}{\rho_P} j_{s,k-1},$$

where M_P and ρ_P are the average molecular weight and density of lithium and products, noting that the sign of j_s is negative.

- This result can be used to calculate the film resistance as

$$R_{\text{film}} = R_{\text{SEI}} + \delta_{\text{film}}/\kappa_P$$

$$R_{\text{film},k} = R_{\text{film},k-1} - \frac{M_P \Delta t}{\rho_P \kappa_P} j_{s,k-1}.$$

- Similarly, we can discretize the capacity equation

$$\frac{\partial Q}{\partial t} = \int_0^{L_n} a_n A F j_s dx$$

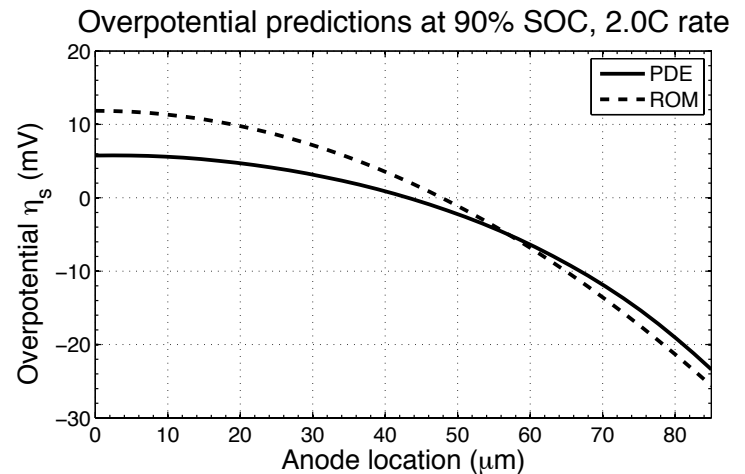
$$Q_k = Q_{k-1} + (a_n A F L_n \Delta t) j_{s,k-1}.$$

7.7: Simulation and results

- A reduced-order model is derived in the aforementioned paper.
- The validity of this reduced-order model depends first on the accuracy of the underlying partial differential equation model, which we assume here to be exact.
- It then depends on how closely the reduced-order approximation of \bar{j}_s matches the exact calculation of \bar{j}_s . In this section, results from both the full and reduced-order models for \bar{j}_s are compared.
- To compare the PDE and reduced-order models, we conducted a series of simulations.
 - In each simulation, the cell was initially at rest.
 - A sudden pulse of current was then applied, and the resulting \bar{j}_s from the PDE model, averaged over a one-second interval subsequent to the pulse, was compared to the computed \bar{j}_s from the ROM.
- To simulate the PDE model, we used COMSOL Multiphysics 3.5a coupled with a MATLAB script to cycle through the series of simulations and analyze results.
- Specifically, each simulation comprised a 1.2 s time interval, where the cell current i_{app} was modeled as a step function, which was applied at $t = 0.2$ s.
- We found that the initial rest interval facilitated convergence of the solution by allowing the PDE solver to adjust its initial conditions before applying the step current.

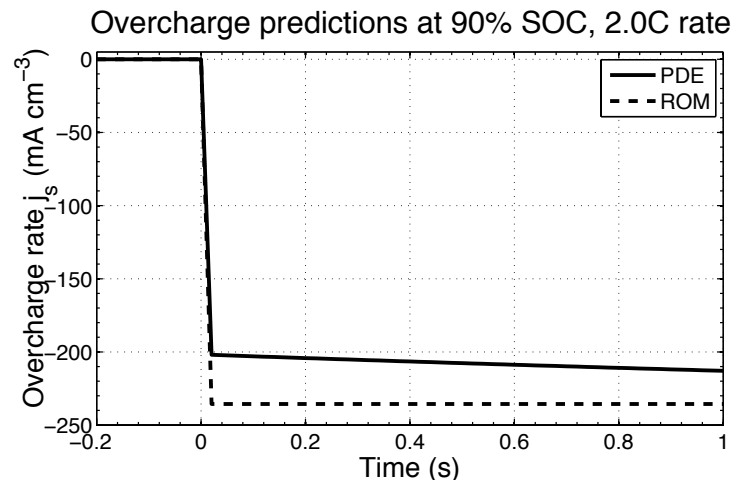
- The cell parameters that we used in the simulations match those used in Arora and are listed in the appendix.
 - The applied current was varied between 0C and 3C in increments of C/33;
 - The initial cell SOC was varied between 0 % and 100 % in steps of 1 %, and
 - Temperature was held constant at 25 °C.
- We found that the adjustable tuning factor $\beta = 1.7$ worked well (this implies the change in electrolyte concentration near the separator changes nearly twice as quickly as it does near the current collector).
- A total of 10 100 simulations were run.
 - As one point of comparison, the set of full-order PDE simulations took approximately 12 hours to complete, utilizing an average of three cores, on an Intel i7 processor, while
 - The set ROM simulations took approximately 21 seconds to complete, utilizing an average of one core on the same machine.
 - The speedup, on a per-simulation per-core basis, is more than 5 000 : 1. This is the primary advantage of the ROM over the PDE model.
- Lithium plating occurs when the side-reaction overpotential is negative ($\eta_s < 0$).

- The figure illustrates the side-reaction overpotential across the negative electrode for this cell model, where $x = 0$ is adjacent to the current-collector and $x = 85 \mu\text{m}$ is adjacent to the separator, immediately following the onset of a charge current pulse.

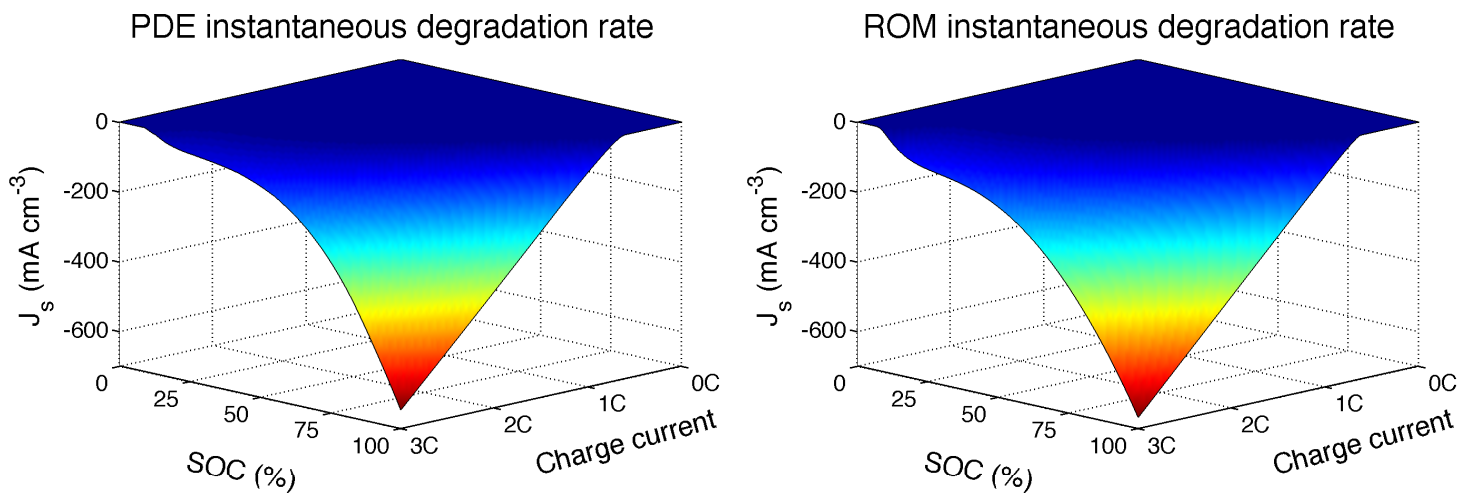


- From the PDE result, we expect lithium deposit to occur between about $x = 42 \mu\text{m}$ and $x = 85 \mu\text{m}$. From the ROM, we expect lithium deposit to occur between $x_0 = 49 \mu\text{m}$ and $x = 85 \mu\text{m}$.

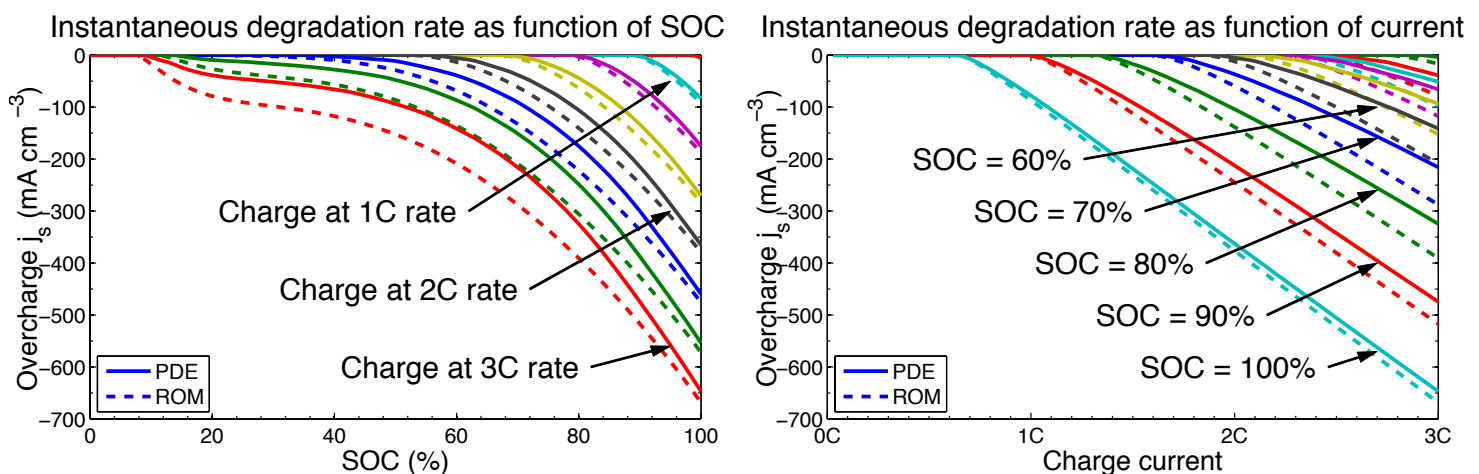
- The figure to the right shows the resulting rate of lithium deposition for the PDE and ROM solutions.



- The time-average deposition rate of the ROM is somewhat higher than the time-average deposition rate of the PDE over the 1 s interval.
- The figures below illustrate the predicted overcharge rates over all scenarios for the PDE and the ROM solutions.

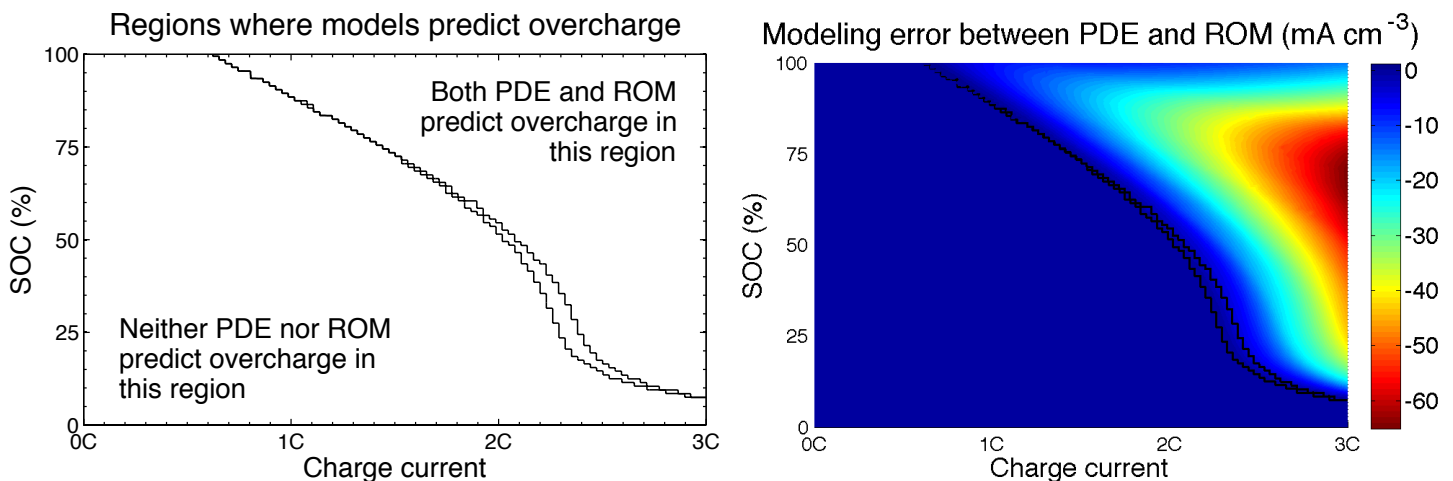


- As expected, deposition is worse at high SOC and high charge rates. The PDE and ROM solutions generally agree very well, with greatest mismatch at high charge rates.
- The figures below show a different view of the results.
 - Cross sections through both the PDE and ROM solution spaces are plotted and compared.



- The left figure shows how the two methods compare where each pair of lines represents a specific charge rate.

- As noted before, but perhaps more clearly seen here, the difference between the PDE and ROM solutions are greatest at high charge rates.
- The right figure shows how the two methods compare where each pair of lines represents a specific initial SOC.
 - The difference is greatest at moderate SOC levels.
- Finally, the figures below illustrate the error between the PDE and ROM solutions in two ways.



- The left frame shows the regions where the two methods agree on whether lithium deposition will occur, and the region where they disagree.
 - The region of disagreement is the very narrow sliver at around 2.4C and 25% SOC, where the ROM predicts overcharge but the PDE does not.
 - Otherwise, the boundaries are identical.

- The right frame shows the error between the solutions, calculated as $\bar{j}_{s,ROM} - \bar{j}_{s,PDE}$. The maximum error is approximately 65 mA cm^{-2} (relative error on the order of 10 %).
- For the purpose of control system design, the results of the left frame are the most important.
- Since lithium deposition is such a severe degradation mechanism, a charging control scheme should avoid ever commanding a control action that would cause any lithium deposition to occur.
- A time-optimal charger, based only on the PDE model of lithium deposition, would select charge pulse current to follow the upper contour in the left frame.
 - This allows the maximum charge rate at any point in time, while causing no lithium plating.
- In comparison, a time-optimal charger, based only on the ROM model of lithium deposition, would select charge pulse current to follow the lower contour in the figure.
 - This will result in somewhat slower charging.
 - But, because the ROM over-predicts the amount of lithium deposition, it will also result in a charging scheme that is conservative, which is a beneficial feature.
- We conducted additional simulations to investigate the effect of pulse length Δt in assumption 1.
- That is, how long can the charge pulse be before the full-order PDE model and the reduced order model results are significantly different?

- We found that pulse lengths less than 10 s are generally well matched, but pulse lengths much greater than 10 s can give significant PDE versus ROM mismatch.
- For long pulse durations, the quasi-static nature of assumption 1 is violated, and a significant offset is noted in actual time-varying ϕ_e versus the at-rest ϕ_e , moving the crossover point of $\eta_s(x, t)$.
- This causes the ROM to under-predict the value of lithium plating computed by the PDE.
- For this reason, we propose that the ROM is of most value for computing current limits in dynamic applications such as hybrid-electric vehicles, where a bias in ϕ_e cannot develop due to the random nature of power demand, but is of less value for controlling full charges, such as for electric vehicle applications.
- We make one final comment regarding efficiency.
 - The speedup of ROM vs. PDE can be much greater than 5 000 : 1 if ROM solutions are pre-computed and stored in a table.
 - Then, “computing” any value of $\bar{j}_{s,ROM}$ would be nearly instantaneous, via table lookup.
- We note that the ROM solution changes as the film resistance changes, but the film resistance changes very slowly.
- The entire table might be updated by the battery management system once per operational period (*e.g.*, once per day), and then utilized throughout that operational period for significant performance gains.

7.8: Optimized controls for power estimation

- We've now seen that there are quite a few causes of cell degradation, and an attempt at modeling two of the more significant mechanisms.
- Much more work remains to be done in this area, first by materials scientists, then by controls engineers.
- But, how to use these models to compute power to slow aging? We look at a few methods next.
- We have seen that none of the cell degradation mechanisms are tied directly to the cell terminal voltage, but rather to internal stress factors.
- Therefore, assuming that degradation mechanisms can be well modeled, it makes more sense to compute power limits based on predicted capacity loss and/or impedance rise than on voltage limits.
- Clearly, there's a lot of work to do before this is practical, but the potential benefits are worth it.
- The next sections of notes very briefly introduce some optimization methods that might be used with the physics-based degradation mechanisms to compute better power limits.

Two problems

- There are (at least) two controls problems to consider.³
- For EV/E-REV/PHEV, the battery pack is charged from an external source:

³ A third, well beyond our scope here: Considering xEV as storage units for the "smart grid," when does it make sense to "lend" energy to the grid? What should be the rental fee charged for allowing energy to be borrowed?

- What is the optimum charge profile?
- Can we “fast charge”?
- For a fixed charge period, what is the best strategy?
- For all xEV, while the car is being driven,
 - What is the maximum charge power that can be maintained over the next ΔT seconds?
 - What is the maximum discharge power that can be maintained over the next ΔT seconds?
- Different kinds of optimized controls may be better for these two problems.

7.9: Plug-in charging

- The plug-in charging problem lends itself well to being solved by a nonlinear programming method.
 - One example is the sequential quadratic programming algorithm, implemented in MATLAB as `fmincon.m`.
- Nonlinear programming is a generic optimization method that attempts to find solutions to problems that can be posed in the framework:

$$x^* = \arg \min f(x), \quad \text{such that} \begin{cases} c(x) \leq 0 & Ax \leq b \\ c_{\text{eq}}(x) = 0 & A_{\text{eq}}x = b_{\text{eq}} \\ lb \leq x & x \leq ub, \end{cases}$$

where $f(x)$ is a function that we wish to minimize by choosing optimum input vector x^* such that

- Nonlinear inequality constraint vector function $c(x) \leq 0$ is satisfied,
- Nonlinear equality constraint vector function $c_{\text{eq}}(x) = 0$ is satisfied,
- Linear inequality constraint vector function $Ax \leq b$ is satisfied,
- Linear equality constraint vector function $A_{\text{eq}}x = b_{\text{eq}}$ is satisfied,
- Bounds $lb \leq x \leq ub$ for all entries in vector x are satisfied

for user-specified $f(x)$, $c(x)$, $c_{\text{eq}}(x)$, A , b , A_{eq} , b_{eq} , lb , and ub .

- We will choose x to be a vector of cell applied current versus time, $f(x)$ to be some estimate of the cell degradation that would be caused by that applied current, and the other functions and matrices to make the problem work.

- For example, we might want to find

$$i^* = \arg \min \sum_{k=0}^{K-1} -J_s(i_k, z_k, T_k)$$

$$\text{such that } \begin{cases} z_{\min} \leq z_k \leq z_{\max} \\ z_K = z_{\text{end}} \\ -I_{\max} \leq i_k \leq I_{\max} \end{cases}$$

$$\text{and } z_k = z_0 - \sum_{j < k} i_j \Delta t / Q.$$

- This states that we want to minimize capacity loss that would be experienced by a cell if we were to start at SOC z_0 and end at SOC z_{end} over a period of K sampling intervals, where current is limited between $\pm I_{\max}$, and SOC is limited between z_{\min} and z_{\max} and the standard SOC equation holds.
- It takes a little work to recast this problem in the right framework, but it's not too bad.
- First, consider the SOC equation. We can write it in vector form as:

$$\begin{bmatrix} z_1 \\ z_2 \\ \vdots \\ z_K \end{bmatrix} = \underbrace{\begin{bmatrix} 1 \\ 1 \\ \vdots \\ 1 \end{bmatrix}}_{CV} z_0 - \frac{\Delta t}{Q} \underbrace{\begin{bmatrix} 1 & 0 & 0 & 0 & \cdots & 0 \\ 1 & 1 & 0 & 0 & \cdots & 0 \\ \vdots & \vdots & \vdots & \vdots & \ddots & \vdots \\ 1 & 1 & 1 & 1 & \cdots & 1 \end{bmatrix}}_{LT} \underbrace{\begin{bmatrix} i_0 \\ i_1 \\ \vdots \\ i_{K-1} \end{bmatrix}}_x.$$

- Notice that the matrix LT is lower-triangular.
- Using this formulation, we can write an equation for the z_K constraint

$$z_K = z_0 - \frac{\Delta t}{Q} \begin{bmatrix} 1 & 1 & 1 & \cdots & 1 \end{bmatrix} x = z_{\text{end}},$$

or, in the prescribed format for `fmincon.m`,

$$\underbrace{\begin{bmatrix} 1 & 1 & 1 & \cdots & 1 \end{bmatrix}}_{A_{\text{eq}}} x = \underbrace{\frac{Q}{\Delta t} (z_0 - z_{\text{end}})}_{b_{\text{eq}}}.$$

- The limit $z_{\min} \leq z_k$ can be written as

$$\begin{bmatrix} 1 \\ 1 \\ \vdots \\ 1 \end{bmatrix} z_{\min} \leq \underbrace{\begin{bmatrix} 1 \\ 1 \\ \vdots \\ 1 \end{bmatrix}}_{CV} z_0 - \frac{\Delta t}{Q} \underbrace{\begin{bmatrix} 1 & 0 & 0 & 0 & \cdots & 0 \\ 1 & 1 & 0 & 0 & \cdots & 0 \\ \vdots & \vdots & \vdots & \vdots & \ddots & \vdots \\ 1 & 1 & 1 & 1 & \cdots & 1 \end{bmatrix}}_{LT} \underbrace{\begin{bmatrix} i_0 \\ i_1 \\ \vdots \\ i_{K-1} \end{bmatrix}}_x$$

$$(CV)(z_{\min} - z_0) \leq -\frac{\Delta t}{Q} (LT) x$$

$$(LT) x \leq \frac{Q}{\Delta t} (CV)(z_0 - z_{\min}).$$

- Similarly, $z_k \leq z_{\max}$ can be written as

$$-(LT)x \leq \frac{Q}{\Delta t} (CV)(z_{\max} - z_0).$$

- Putting the last two constraints together gives

$$\underbrace{\begin{bmatrix} LT \\ -LT \end{bmatrix}}_A x \leq \underbrace{\frac{Q}{\Delta t} \begin{bmatrix} (CV)(z_0 - z_{\min}) \\ (CV)(z_{\max} - z_0) \end{bmatrix}}_b.$$

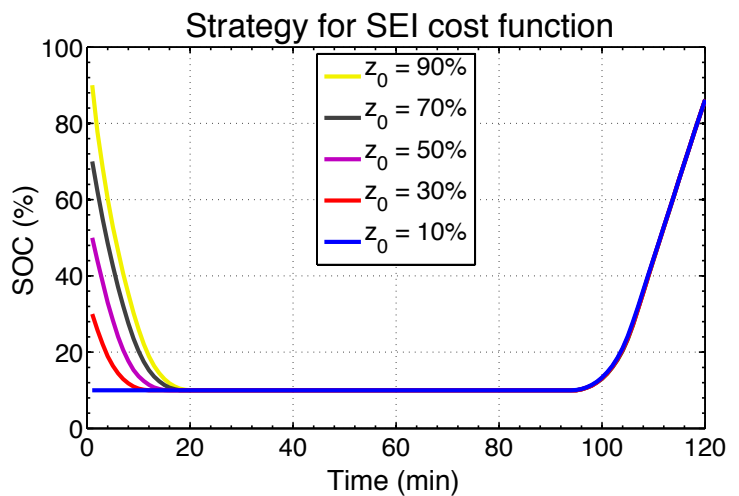
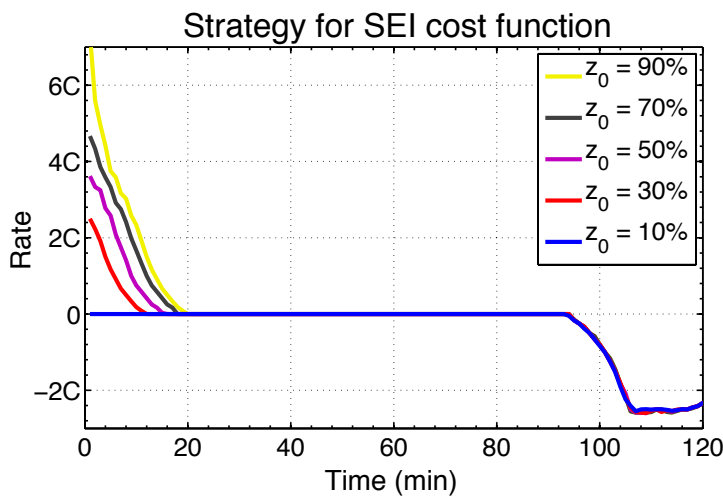
- The constraints on input current can be satisfied by setting

$$lb = -I_{\max}(CV), \quad \text{and} \quad ub = I_{\max}(CV).$$

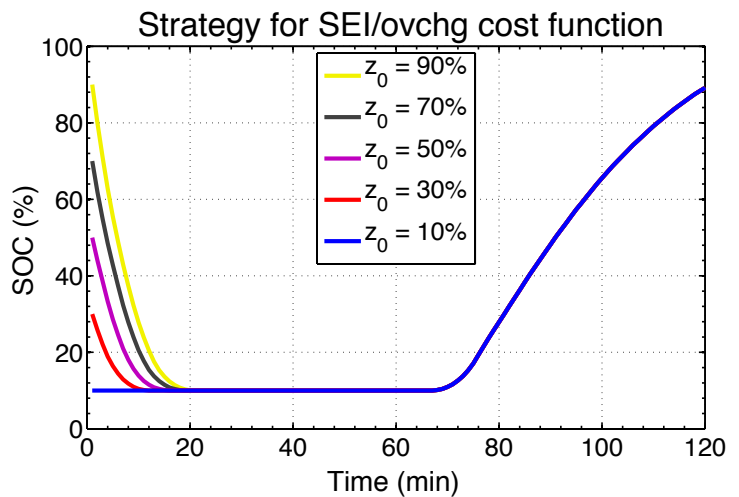
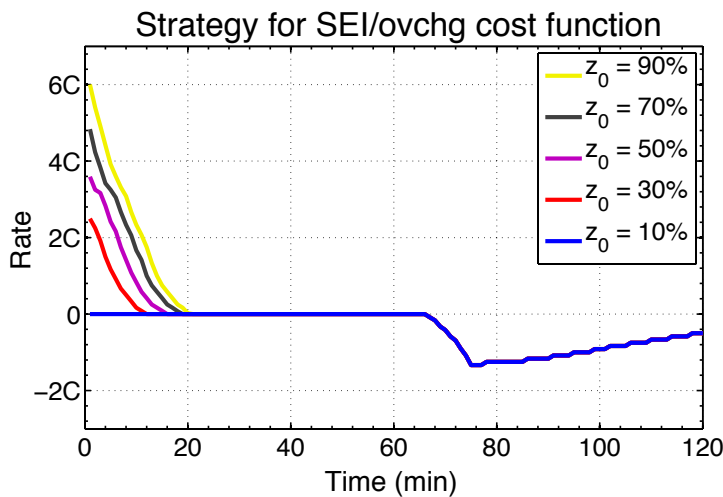
- Then, all that's left is to specify the cost function $f(x)$. (There are no nonlinear constraints in this problem.)
- Given what we've seen so far, we might consider j_s to represent the SEI growth model, or the overcharge model, or the sum of both.

7.10: Fast-charge example

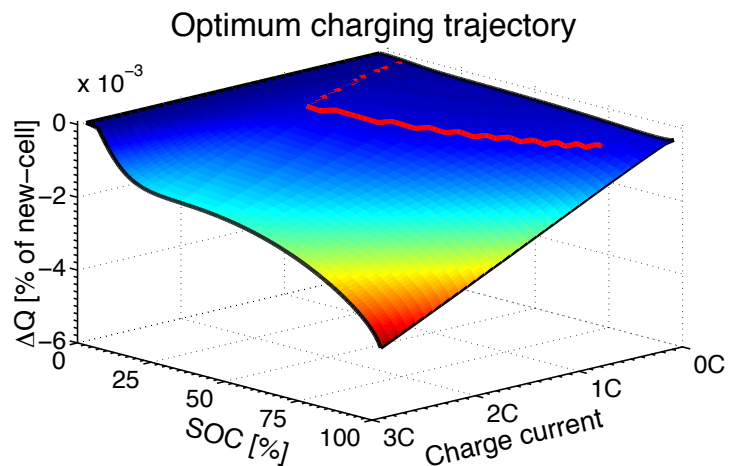
- We designed optimized controllers to investigate charging strategies using the degradation models generated to date.
- In the first controls scenarios, the cell was initially at a SOC value between 10 % and 90 %, and the charger was required to optimally charge the cell to 90 % over a period of two hours.
- SOC was not allowed outside the range of 10 % to 90 %, but current was unconstrained.
- We first looked at using only the SEI-growth degradation model in the control strategy:

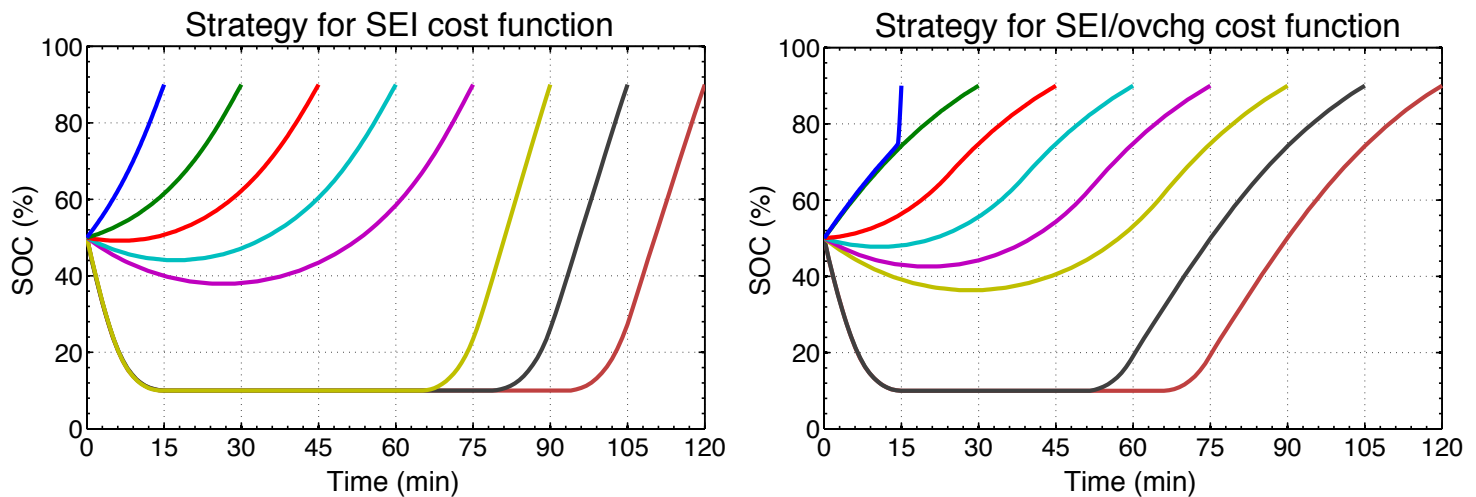


- The optimum charging strategy for this model is to quickly discharge the cell to the minimum SOC, wait “as long as possible” and then quickly charge the cell to the desired SOC.
- The cost of discharging plus charging turns out to be less than the cost of maintaining a high SOC for an extended period of time(!)
- We then looked at using the SEI plus the overcharge cost functions added together:



- These are qualitatively similar, but different in some details.
 - In particular, the final charge event is at a much lower rate, and
 - Charge current tapers off at high SOC to avoid lithium plating.
- For grins, we overlay optimum SEI plus overcharge charging profile on top of the degradation function.
- Optimization method automatically avoids the “cliff” where degradation starts to get much worse.
- Third, we looked at fast charging strategies, with results plotted below.
- The cell was at an initial SOC of 50 %, then was allowed 15, 30, 45, 60, 75, 90, 105, or 120 minutes to charge to 90 %.
- Strategies using the SEI cost function and the combined SEI plus overcharge cost function are shown.





- Again, they are similar, but not identical.
 - If sufficient time is granted, the charger will discharge the cell to the minimum allowed SOC, and then charge the cell.
 - If less time is granted, the charger will only partially discharge the cell before charging.
 - If even less time is granted, charger charges cell immediately.

7.11: Dynamic power calculation

- As discussed in Ch. 6, the goals of dynamic power calculation are:
 - a) Discharge power: Based on present battery-pack conditions, estimate the maximum discharge power that may be maintained constant for ΔT seconds without violating pre-set design limits on cell voltage, SOC, maximum design power, or current.
 - b) Charge power: Based on present battery-pack conditions, estimate the maximum battery charge power that may be maintained constant for ΔT seconds without violating pre-set design limits on cell voltage, SOC, maximum design power or current.
- As before, we handle this problem by looking for the maximum dis/charge current the cell can withstand, and then convert that value to power by multiplying by voltage.
- Unlike before, we now consider degradation mechanisms to be the limiting factor, rather than cell terminal voltage limits.
- The method proposed here is not yet thoroughly tested, but with some work should give good results.
- It is closely related to a control-system design paradigm called Model Predictive Control (MPC). The idea is to:
 - Determine an N -length sequence of control signals, using a model of the system to be controlled to predict future system performance, that will cause the system's controlled variables to converge toward desired values;
 - Implement only the first of these N signals;
 - Repeat.

- This allows us, for example, to predict a constant-current input that would not violate limits and would optimize a cost function if applied for the full ΔT seconds (N sample periods), but only implement the first of these, then repeat.
- Standard MPC is a little different from what we will look at here:
 - MPC reformulates the system model to use Δu_k as the input signal rather than u_k ;
 - This formulation implicitly adds an integrator to the dynamics, which is good for control, but is unnecessary for power estimation.
 - Also, seems appropriate for set-point control: when $\Delta u_k = 0$, then u is a constant and y approaches a steady-state constant.
 - ◆ Again, not necessary for power estimation.
 - Also, standard MPC does not allow the state-space model to have a direct feedthrough “ D ” term, which we need here.
- We’ll use a similar idea to MPC, leading up to the same form of quadratic optimization used by MPC.
- The system model we assume is:

$$x_{k+1} = Ax_k + Bu_k$$

$$y_k = Cx_k + Du_k,$$

where y_k are the performance variables that we would like to control to some limit, or to maintain within some hard constraints.

- That is, y_k may be different from the normal system outputs that we have called y_k in the past.

- Define the vectors:

$$Y = \begin{bmatrix} y_k & y_{k+1} & \cdots & y_{k+N} \end{bmatrix}^T \quad \text{and} \quad U = \begin{bmatrix} u_k & u_{k+1} & \cdots & u_{k+N} \end{bmatrix}^T .$$

- Then, we can write,

$$\underbrace{\begin{bmatrix} y_k \\ y_{k+1} \\ y_{k+2} \\ \vdots \\ y_{k+N} \end{bmatrix}}_Y = \underbrace{\begin{bmatrix} C \\ CA \\ CA^2 \\ \vdots \\ CA^N \end{bmatrix}}_F x_k + \underbrace{\begin{bmatrix} D & & & 0 \\ CB & D & & \\ CAB & CB & & \\ \vdots & \vdots & \ddots & \\ CA^{N-1}B & CA^{N-2}B & \cdots & D \end{bmatrix}}_\Phi \underbrace{\begin{bmatrix} u_k \\ u_{k+1} \\ u_{k+2} \\ \vdots \\ u_{k+N} \end{bmatrix}}_U$$

$$Y = F x_k + \Phi U .$$

- Now, we define a cost function that we wish to optimize:

$$\begin{aligned} J &= (R_s - Y)^T Q (R_s - Y) + U^T R U \\ &= (R_s - [F x_k + \Phi U])^T Q (R_s - [F x_k + \Phi U]) + U^T R U \\ &= R_s^T Q R_s - R_s^T Q F x_k - R_s^T Q \Phi U \\ &\quad - x_k^T F^T Q R_s + x_k^T F^T Q F x_k + x_k^T F^T Q \Phi U \\ &\quad - U^T \Phi^T Q R_s + U^T \Phi^T Q F x_k + U^T \Phi^T Q \Phi U + U^T R U . \end{aligned}$$

- To simplify this, note that each term is a scalar, and hence equal to its own transpose:

$$\begin{aligned} J &= [R_s^T Q R_s - 2R_s^T Q F x_k + x_k^T F^T Q F x_k] \quad (\text{not a function of } U) \\ &\quad + 2[x_k^T F^T Q \Phi - R_s^T Q \Phi] U \\ &\quad + U^T [\Phi^T Q \Phi + R] U . \end{aligned}$$

- Let,

$$H = 2[\Phi^T Q \Phi + R]$$

$$f^T = 2(x_k^T F^T Q \Phi - R_s^T Q \Phi).$$

- Then,

$$J = \frac{1}{2}U^T H U + f^T U + \text{constant}.$$

- Further, we can put constraints on Y via

$$Y_{\min} \leq F x_k + \Phi U \leq Y_{\max},$$

which can be written as

$$\Phi U \leq [Y_{\max} - F x_k]$$

$$-\Phi U \leq [F x_k - Y_{\min}],$$

which can both be combined in the matrix inequality

$$\underbrace{\begin{bmatrix} \Phi \\ -\Phi \end{bmatrix}}_{A_{\text{ineq}}} U \leq \underbrace{\begin{bmatrix} Y_{\max} - F x_k \\ F x_k - Y_{\min} \end{bmatrix}}_{b_{\text{ineq}}},$$

or, $A_{\text{ineq}} U \leq b_{\text{ineq}}$.

- So, we now have defined vectors/matrices H , f^T , A_{ineq} , and b_{ineq} that match a quadratic programming problem, which is:

$$U^* = \arg \min \frac{1}{2}U^T H U + f^T U$$

such that

$$A_{\text{ineq}} U \leq b_{\text{ineq}}.$$

- In MATLAB, the solution is found via `quadprog.m`.

- Note, we can use

$$U = \begin{bmatrix} 1 & 1 & 1 & \cdots & 1 \end{bmatrix}^T u$$

to make a fast single-variable optimization problem, to give us the maximum dis/charge current value that would apply to all times.

- But, what values to use?
 - Reference R_s value for model SOC state on charging set to 1.0;
 - Reference R_s value for model SOC state on discharging set to 0.0;
 - Need to define other reference variables for soft constraints to minimize degradation mechanisms (how?);
 - Hard constraints must be set to prohibit lithium plating in the negative electrode.

Where from here?

- We've reached the edge of what we presently know how to do for battery management.
- There's plenty of work yet to do:
 - How do we efficiently implement the optimized power controls, and how do we tune to accommodate various aging mechanisms and cost tradeoffs?
 - How do we perform system identification of physics-based model parameters to give a good enough model to match a real cell well?
 - How do we model new degradation mechanisms in efficient ways, for implementation in embedded systems?
- And many more we haven't even thought of yet.
- I hope some of this material has sparked your imagination, and I hope you will be able to contribute to making battery management systems of the future even better!

Appendix: Parameters used for SEI simulations

| Symbol | Units | Neg. electrode | Separator | Pos. electrode |
|-------------------------|--------------------------------------|------------------------|-----------------------|------------------------|
| L | μm | 88 | 20 | 80 |
| R | μm | 2 | - | 2 |
| A | m^2 | 0.0596 | 0.0596 | 0.0596 |
| σ | S m^{-1} | 100 | - | 100 |
| ε_s | - | 0.49 | - | 0.59 |
| ε_e | - | 0.485 | 1 | 0.385 |
| brug | - | 4 | - | 4 |
| c_s^{max} | mol m^{-3} | 30 555 | - | 51 555 |
| c_e^0 | mol m^{-3} | 1 000 | 1 000 | 1 000 |
| $\theta_{i,\text{min}}$ | - | 0.03 | - | 0.95 |
| $\theta_{i,\text{max}}$ | - | 0.886 | - | 0.487 |
| D_s | $\text{m}^2 \text{s}^{-1}$ | 3.9×10^{-14} | - | 1.0×10^{-14} |
| D_e | $\text{m}^2 \text{s}^{-1}$ | 7.5×10^{-10} | 7.5×10^{-10} | 7.5×10^{-10} |
| t_+^0 | - | 0.363 | 0.363 | 0.363 |
| k | $\text{A m}^{5/2} \text{mol}^{-3/2}$ | 4.854×10^{-6} | - | 2.252×10^{-6} |
| α_a | - | 0.5 | - | 0.5 |
| α_c | - | 0.5 | - | 0.5 |
| U_s^{ref} | V | 0.4 | - | - |
| $i_{0,s}$ | A m^{-2} | 1.5×10^{-6} | - | - |

Appendix: Parameters used for overcharge simulations

| Symbol | Units | Neg. electrode | Separator | Pos. electrode |
|--------------------|--------------------------------------|-----------------------|-----------------------|-----------------------|
| L | μm | 85 | 76.2 | 179.3 |
| R | μm | 12.5 | - | 8.5 |
| A | m^2 | 1 | 1 | 1 |
| σ | S m^{-1} | 100 | - | 3.8 |
| ε_s | - | 0.59 | - | 0.534 |
| ε_e | - | 0.36 | 1 | 0.416 |
| κ_e | S m^{-1} | 0.2875 | 0.2875 | 0.2875 |
| brug | - | 1.5 | - | 1.5 |
| c_s^{\max} | mol m^{-3} | 30 540 | - | 22 860 |
| c_e^0 | mol m^{-3} | 1 000 | 1 000 | 1 000 |
| $\theta_{i,\min}$ | - | 0.10 | - | 0.95 |
| $\theta_{i,\max}$ | - | 0.90 | - | 0.175 |
| D_s | $\text{m}^2 \text{s}^{-1}$ | 2.0×10^{-14} | - | 1.0×10^{-13} |
| D_e | $\text{m}^2 \text{s}^{-1}$ | 7.5×10^{-11} | 7.5×10^{-11} | 7.5×10^{-11} |
| t_+^0 | - | 0.363 | 0.363 | 0.363 |
| k | $\text{A m}^{5/2} \text{mol}^{-3/2}$ | 2×10^{-6} | - | 2×10^{-6} |
| α_a | - | 0.5 | - | 0.5 |
| α_c | - | 0.5 | - | 0.5 |
| $\alpha_{a,s}$ | - | 0.3 | - | - |
| $\alpha_{c,s}$ | - | 0.7 | - | - |
| U_s^{ref} | V | 0.0 | - | - |
| R_{SEI} | $-\text{m}^2$ | 0.002 | - | - |
| $i_{0,s}$ | A m^{-2} | 10 | - | - |